FEBS Letters 587 (2013) 1385–1391

FEBS Letters
journal homepage: www.FEBSLetters.org

Partitioning and confinement of GM1 ganglioside induced by amyloid aggregates

Martino Calamai [a,b,*], Francesco S. Pavone [b,c,d,e]

[a] CNR Neuroscience Institute, Pisa, Italy
[b] European Laboratory for Non-Linear Spectroscopy, Sesto Fiorentino, Italy
[c] Department of Physics and Astronomy, University of Florence, Sesto Fiorentino, Italy
[d] National Institute of Optics, National Research Council, Florence, Italy
[e] International Center of Computational Neurophotonics, Sesto Fiorentino, Italy

ARTICLE INFO

Article history:
Received 4 January 2013
Revised 22 February 2013
Accepted 7 March 2013
Available online 20 March 2013

Edited by Jesus Avila

Keywords:
GM1
Aβ1–42
Amylin
Single particle tracking
Lateral diffusion

ABSTRACT

Growing evidence shows that GM1 ganglioside is involved in amyloid deposition and toxicity. By means of real-time single particle tracking, we show that amyloid oligomers and aggregates formed by Aβ1–42 and amylin, two peptides associated, respectively, with the development of Alzheimer's disease and type II diabetes, interact with GM1 and decrease dramatically its lateral diffusion on the plasma membrane of living neuroblastoma cells. The confinement of GM1, a constituent of membrane rafts involved in neuroprotection, at the level of both types of amyloid aggregates can interfere with cell signaling pathways and contribute to the loss of neuroprotection.

1. Introduction

Neuronal impairment in Alzheimer's disease (AD) is currently attributed to a complex cascade of events triggered by the interaction of amyloid oligomers, constituted primarily by Aβ1–42 peptide, with the plasma membrane [1]. Amongst the variety of toxic mechanisms proposed, one involves the binding of amyloid species to GM1 gangliosides [2–6]. GM1 takes part into the formation of membrane rafts, dynamic and specialized membrane microdomains responsible for the compartmentalization of cellular processes such as signalling and protein trafficking [7,8]. Altered distribution of GM1 and GM2 gangliosides has been recently found in AD brains [9]. The interaction with GM1 has been demonstrated to be a crucial factor also in mediating the aggregation and toxicity of other amyloidogenic proteins and peptides [10–12], such as amylin (also known as human islet polypeptide, hIAPP), whose aggregation and binding to the plasma membrane is thought to be the main factor determining the death of pancreatic β-cells in type II diabetes [13]. In particular, in vitro experiments show that the aggregation and seeding of Aβ and amylin peptides on synthetic membranes are enhanced in the presence of GM1 [10,14,15], as well as in vivo studies demonstrate increased assembly at the level of membrane rafts [12,16,17]. Conversely, GM1 is fundamental in mediating the binding of preformed Aβ oligomers and amylin aggregates to synthetic lipid vesicles and causing their subsequent permeabilitzation [12,18]. Exogenously applied oligomeric Aβ1–42 has been shown to accumulate on the membrane of cultured neurons at the level of rafts enriched in GM1 [17]. Nevertheless, experiments providing compelling evidence of interaction between Aβ oligomers and GM1 in living cells are still missing. The consistent, although sometimes conflicting, body of literature on the interaction of GM1 with amyloid species relies on averaged results obtained using bulk methods. In this case, many important details can be missed and only the most prominent features are eventually taken into account.

Here we take advantage of single particle tracking (SPT) techniques to monitor in real-time in living cells the dynamics of GM1 following the binding of amyloid aggregates of Aβ1–42 and amylin to the plasma membrane. We demonstrate that a direct interaction takes place in vivo, heavily affecting the diffusion properties of a subpopulation of GM1 molecules. Our results might imply an additional mechanism of toxicity, where amyloid aggregates alter cellular processes dependent on membrane raft mobility and clustering.

* Corresponding author at: LENS, European Laboratory for Non-Linear Spectroscopy, University of Florence, Via Nello Carrara 1, I 50019 Sesto-Fiorentino, Florence, Italy. Fax: +39 055 4572451.
E-mail address: calamai@lens.unifi.it (M. Calamai).

0014-5793/$36.00
http://dx.doi.org/10.1016/j.febslet.2013.03.014

2. Materials and methods

2.1. Cell culture

Human SH-SY5Y neuroblastoma cells were obtained from A.T.C.C. (Manassas, VA) and cultured in 1:1 DMEM/F-12 supplemented with 10% FBS and 1.0% antibiotics. Cell cultures were maintained in a 5.0% CO_2 humidified atmosphere at 37 °C and grown until 80% confluence. Cells were used for a maximum of 20 passages.

2.2. Oligomers preparation and cells treatment

Aβ1–42 (A9810) and amylin (D2162) were purchased from Sigma. Amylin or Aβ1–42 peptides were initially incubated in hexafluoroisopropanol (HFIP) at room temperature for 1 h. The HFIP was evaporated under a gentle stream of N_2. Dried peptide aliquots were dissolved in anhydrous DMSO to a final concentration of 5.0 mM, diluted into ice-cold phenol red-free F12 medium to 100 μM and incubated at 4 °C for 24 h. Aβ1–42 and amylin samples were transferred directly to the cell medium to a final concentration of 10 μM monomer equivalent for 1 h at 37 °C.

2.3. Immunolabeling

Following standard protocols, cells previously exposed to amyloid aggregates were fixed in 4% paraformaldehyde for 10 min at room temperature, and then blocked with bovine serum albumin (BSA, 1 mg/ml, Sigma–Aldrich). Mouse monoclonal anti-Aβ (β-Amyloid DE2B4, Santa Cruz Biotechnology Inc., 1:100 dilution) and anti-amylin (Amylin R10/99, Santa Cruz Biotechnology Inc., 1:50 dilution) antibodies were used as primary antibodies (50 min). Alexa 568 anti-mouse antibodies (Invitrogen) were used as secondary antibodies at 1:500 dilution (30 min). No labeling was observed when cells were incubated in the absence of aggregates. GM1 was labeled by incubating cells for 20 min with 10 μg/ml biotinylated ctxb (C9972, Sigma) and subsequentely with streptavidin-Atto 488 (Atto Tec) at 1:500 dilution (20 min). Finally, we incubated cover slips for 1 min with 1 μg/ml Hoechst 33342 (Invitrogen). Washing was performed between each step in PBS. The cover slips were mounted on glass microscope slides with a Mowiol 4-88 solution (9% Mowiol w/w, 22.7% glycerol w/w, 0.2 M Tris–HCl, pH 8.5, 3 mM NaN_3.

Cells were monitored with a Nikon Eclipse TE300 inverted microscope equipped with a Nikon Plan-Apo 60XA/1.40 n.a. DICH WD 0.21 oil immersion objective. Excitation light was provided by a mercury lamp (Hg 100 W). Fluorescence signal was detected by a Hamamatsu Photonics K.K. Japan high sensitivity silicon-intensified target (SIT) camera, coupled to a Hamamatsu Argus Image Processor and a Hamamatsu C2400 camera controller. Digital images were captured using a custom-made Virtual Instrument on Labview 7.1.

2.4. PLA

In situ Proximity Ligation Assay (PLA) was performed with Duolink kit (Olink, Bioscience) with minor modifications at the level of primary antibody labeling. Basically, two primary antibodies raised in different species recognize the target antigen or antigens of interest. Species-specific secondary antibodies, called PLA probes, each with a unique short DNA strand attached to it, bind to the primary antibodies. When the PLA probes are in close proximity (<40 nm), the DNA strands can interact through a subsequent addition of two other circle-forming DNA oligonucleotides. After joining of the two added oligonucleotides by enzymatic ligation, they are amplified via rolling circle amplification using a polymerase. After the amplification reaction, several-hundredfold replication of the DNA circle has occurred, and labeled complementary oligonucleotide probes highlight the product. The resulting high concentration of fluorescence in each single-molecule amplification product is easily visible as a distinct bright dot. Here, cells previously exposed to amyloid aggregates were fixed following the protocol above and incubated with anti-Aβ1–42 or anti-amylin (1:100 or 1:50, respectively) for 20 min, and anti-mouse PLA probe. Regarding the anti-rabbit PLA probe the labeling procedure was more elaborated but still feasible. Cells were incubated for 10 min with 10 μg/ml biotinylated ctxb, subsequentely with 10 μg/ml streptavidin (Invitrogen) for 1 min, with biotinylated anti-rabbit Fab antibodies (1:400, Abcam) for 15 min, then with a randomly chosen rabbit antibody (in this case we used anti-hypf-N, 1:100), and finally with the anti-rabbit PLA probe.

2.5. Single particle imaging and tracking

Quantum dots (QDs) labeling and live imaging has been extensively described in [19]. Briefly, living cells previously exposed to amyloid aggregates were incubated in phenol red-free Leibovitz's L-15 medium 10% FBS at 37 °C first with anti-Aβ1–42 or anti-amylin (1:100 or 1:50, respectively) for 20 min, then for 5 min with anti-mouse Alexa 488 (1:500) and 10 μg/ml biotinylated ctxb, and finally with streptavidin QDs (Invitrogen) in QD binding buffer for 1 min. QDs emitting at 655 nm were used at a 1:10 000 dilution. Cells were monitored with a custom-made wide-field epifluorescence microscope equipped with an oil-immersion objective (Nikon Plan Apo TIRF 60×/1.45), a Reliant 150 Select argon ion laser (excitation line 488 nm) and a heating chamber. A FF499-Di01-25 dichroic, and FF01-655/15-25 (for QDs) and FF01-530/43-25 (for Alexa 488) emission filters (Semrock) were used. 250 or 100 consecutive frames were acquired with an integration time of 330 ms, respectively, with an Electron Multiplying Charge-Coupled device camera PI-Max (Roper Scientific) using WinView (PI Acton, Roper Scientific). Recording sessions did not last more than 30 min.

Tracking of single QDs, which were identified by their fluorescence intermittence, was performed with MATLAB (MathWorks, Natick, MA) using a homemade macro that accounts for blinking in the fluorescence signal [19–21]. In brief, the method consisted of two main steps, applied successively to each frame of the sequence. First, fluorescent spots were detected by cross-correlating the image with a Gaussian model of the Point Spread Function. A least-squares Gaussian fit was applied (around the local maximum above a threshold) to determine the center of each spot with a spatial accuracy of 10–20 nm (depending on the signal-to-noise ratio). Second, QD trajectories were assembled automatically by linking, from frame to frame, the centres of the fluorescent spots likely coming from the same QD. The association criterion was based on the assumption of free Brownian diffusion and took into account short blinking events. After completion of the process, a manual association step was performed, in which QD trajectories of maximal length were assembled from smaller fragments separated by longer blinking events that were not taken into account by the automatic linking procedure. A high concentration of pentavalent B subunit of cholera toxin can in principle induce crosslinking of GM1 [22]. For SPT experiments, however, we incubated the cells with ctxb for times shorter than for standard immunolabeling experiments, thus obtaining a lower level of labeling. The concentration of strep-QDs was largely in excess with respect of biotin-ctxb. Most if not all the ctxb molecules bound to the plasma membrane are therefore expected to be labeled. In our analysis we only monitored the dynamics of all the blinking QDs, indicative of single, not crosslinked, ctxb molecules, and avoided permanently

"on" QDs, possibly deriving from multiple ctxb crosslinked with GM1.

2.6. Quantitative analysis of diffusion coefficient

The mean square displacement (MSD) analysis allows to calculate the initial diffusion coefficient (D) of each particle [19,21]. Briefly, physical parameters can be extracted from each trajectory ($x(t)$, $y(t)$) by computing the MSD [23], determined from the following formula:

$$\mathrm{MSD}(ndt) = \frac{1}{N-n}\sum_{i=1}^{N-n}\left[\left(x_{(i+n)} - x_i\right)^2 + \left(y_{(i+n)} - y_i\right)^2\right]$$

where x_i and y_i are the coordinates of a particle on frame i, dt is the time between two successive frames, N the total number of frames of the trajectory and ndt the time interval over which the displacement is averaged. This function enables the analysis of the lateral dynamics on short (initial diffusion coefficient) and long (types of motion) time scales. Different types of motion can be distinguished from the time dependence of the MSD [23]. The initial diffusion coefficient (D) is determined by fitting the initial 2–5 points of the MSD against time plot with $\mathrm{MSD}(t) = 4D_{2-5}\,t + b$. The cumulative probability $C(d)$ of D defines the probability that D is less that d. We compared cumulative probability distributions and median instead of mean values because D values were spread over four orders of magnitude.

Images were thresholded with ImageJ software, creating binary masks corresponding to amyloid aggregates.

2.7. Position vector analysis

The position vector (r) is defined as:

$$r_i = \left(x_i^2 + y_i^2\right)^{1/2}$$

2.8. Statistical analysis

Comparisons between the different cumulative distributions were performed by Kolmogorov–Smirnov test. A P value <0.05 was considered statistically significant. SPT data ($52 > n > 370$, for each condition) were collected from more than 10 cells from at least three independent experiments.

3. Results

3.1. Co-localization of GM1 and amyloid aggregates

The protocol used in this study has been largely used and leads the formation of toxic amyloid aggregates conformationally similar to those found in human AD brains [4,13,24,25]. Under these conditions, Aβ1–42 displays mostly an oligomeric conformation, while amylin form large aggregates in addition to oligomers [25,26]. Following a previous protocol [26], neuroblastoma SH-SY5Y cells were incubated for 1 h in the presence of 1–10 μM (monomer concentration) preformed amyloid aggregates.

We first investigated the interaction between pre-aggregated amylin and GM1 following a standard immunofluorescence protocol, where a primary antibody is coupled to a secondary fluorescent antibody. Amylin was detected using a primary anti-amylin antibody and a secondary Alexa 568 antibody, while GM1 molecules were subsequently labeled with the biotinylated cholera toxin B subunit (ctxb) and streptavidin Atto-488. As expected, amylin forms large aggregates and GM1 shows a diffuse pattern (Fig. 1A). Due to the homogeneous distribution of GM1 molecules it would be inaccurate to claim, based on these observations, that these co-localize with amylin aggregates. We therefore performed in situ Proximity Ligation Assay (PLA), a more stringent method designed to detect the proximity of two distinct target molecules down to 30–40 nm. Basically, dual recognition of target proteins by pairs of affinity probes generates an amplifiable DNA reporter molecule that is subsequently labeled and serves as a surrogate marker for interacting proteins. Single events of proximity are consequently detected as spots. In the case of amylin, the clustering of the spots was very similar to the shape of fluorescently labeled amylin aggregates (Fig. 1B), suggesting that the GM1 molecules are spatially very close to amylin.

In agreement with previous results, Aβ1–42 oligomeric species bound to the plasma membrane were detected as small punctae following standard indirect immunolabeling with anti-Aβ1–42 and anti-mouse Alexa 568 (Fig. 1C). Also in this case, the uniform distribution of GM1 prevented us to draw any conclusion based on qualitative co-localization with Aβ1–42. By contrast, the PLA approach allowed us to selectively highlight single events of proximity of GM1 and Aβ1–42 molecules (Fig. 1D). The distribution and shape of the PLA signal reflected those of Aβ1–42 oligomers labeled with Alexa 568. The approach based on PLA represents a notable difference from other previously published papers that rely on merged images of GM1 and amyloid aggregates immunolabeled with standard fluorophores to claim an interaction [12,16,17].

These results clearly demonstrate that GM1 and amyloid aggregates formed by amylin and Aβ1–42 are located in very close proximity.

3.2. Single GM1 molecules switch type of motion upon interaction with amyloid aggregates

GM1 mobility has already been the subject of single particle tracking experiments (SPT) [27–29]. Its membrane dynamics has been studied extensively, and therefore we choose to perform SPT experiments to search for a more direct proof of interaction between GM1 and amyloid aggregates. Notably, the mobility of GM1 is not influenced by the size of QDs [27]. At the level of nano-sized probes, the mobility of membrane proteins is rather dependent on the membrane viscosity, which is several order of magnitude greater than that of the extracellular medium [30]. Neuroblastoma SH-SY5Y cells exposed to amylin aggregates were surface labeled with biotin cxtb/QDs 655 and anti-amylin/anti-rabbit alexa 488. During our recordings, we were able to detect real-time changes in GM1 mobility after interaction with amylin (Fig. 2A–D). We discovered that GM1 molecules moving randomly on the plasma membrane switched their motion from brownian to confined once in close proximity of amylin aggregates. This sudden change of mobility is indicative of interaction, as reported in the case of other proteins, such as the scaffolding protein gephyrin and the glycine receptor [31,32].

Switches of motion from brownian to confined were also found when monitoring single GM1 molecules in correspondence of Aβ1–42 oligomers (Fig. 2E–H), which we have previously shown displaying a limited mobility [26].

These results show that a change in dynamic behaviour occurs when GM1 molecules approach amyloid aggregates.

3.3. Confined mobility of GM1 over amyloid aggregates

GM1 molecules switching type of motion represent rare events. Most of the molecules observed during each recording session were found to follow either confined or brownian motion. To quantify to which extent amyloid aggregates could affect the lateral diffusion of GM1 molecules, we compared the diffusion coefficients (D) of GM1 in the absence and presence of the aggregates (Fig. 3A and Table 1). The median D value of GM1 in control condi-

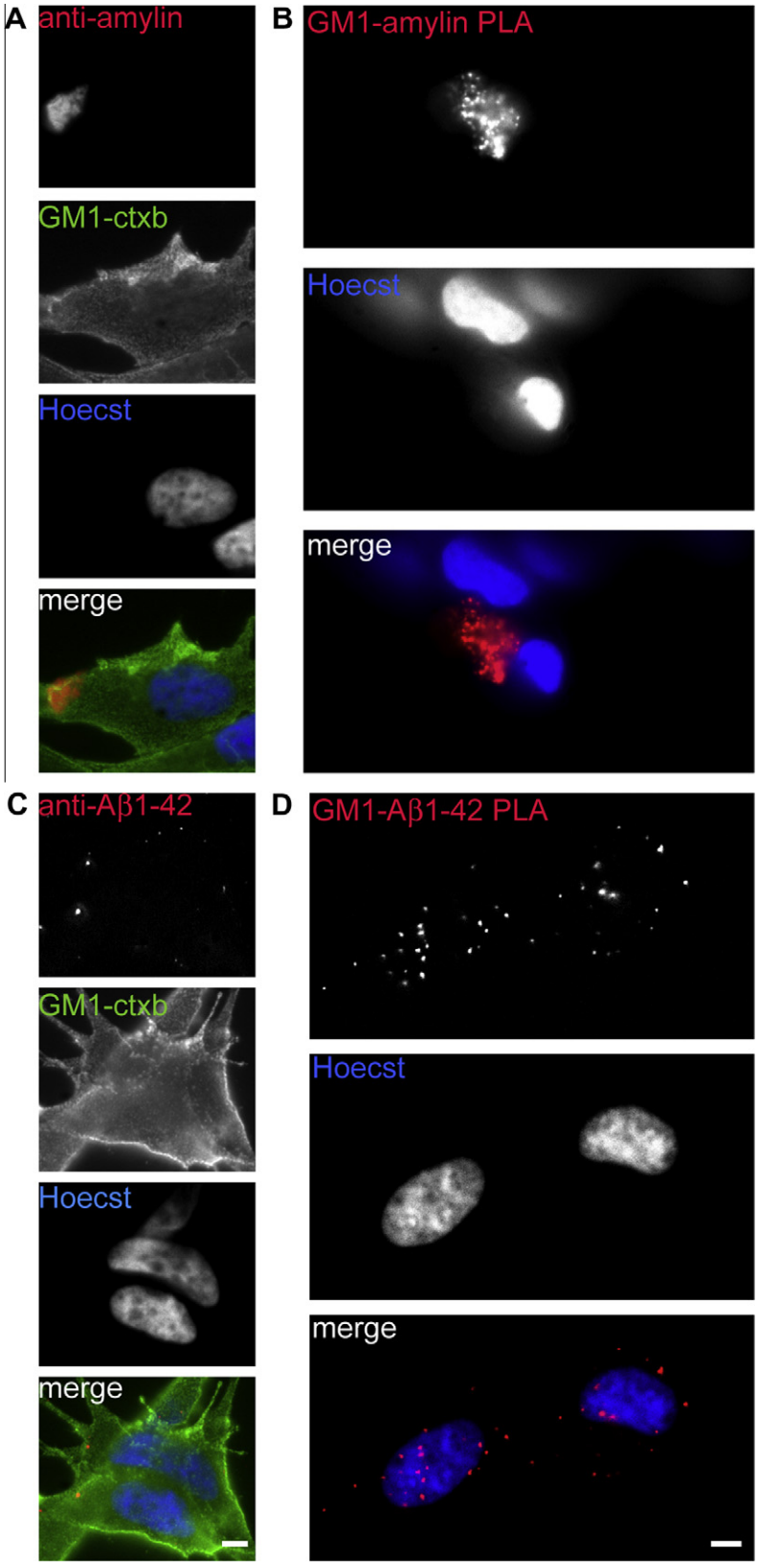

Fig. 1. Close proximity of GM1 and amyloid aggregates. Neuroblastoma cells incubated for 1 h with preformed amylin aggregates (A and B) or Aβ1–42 oligomers (C and D) were fixed and labeled with anti-amylin (A) or anti-Aβ1–42 (C), respectively, and secondary Alexa 568 conjugated antibodies (red). GM1 was detected using biotin-ctxb coupled to streptavidin-Atto 488 (A and C, green). The close proximity of amyloid aggregates and GM1 was highlighted by in situ PLA co-localization assay (Duolink), a technique based on the hybridization of DNA strands from two different specific probes with circle forming oligonucleotides, rolling circle amplification and labeling (B and D). The spot-like fluorescence signal that is generated is present only if GM1 and amylin aggregates (B), or Aβ1–42 oligomers (D), are situated within a theoretical distance of 30–40 nm of each other. Scale bar, 10 μm.

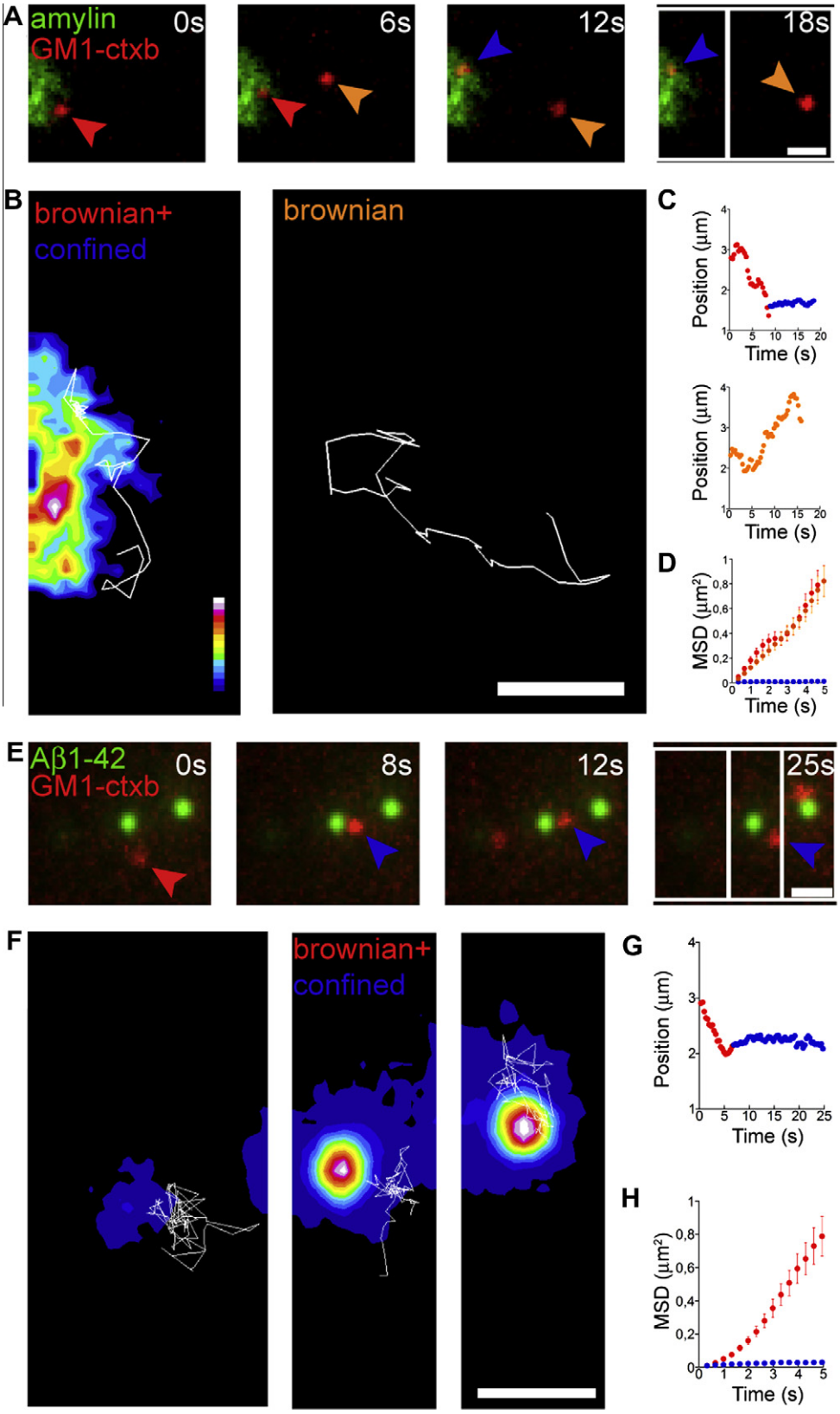

Fig. 2. Real time changes of GM1 mobility in correspondence of amyloid aggregates. Living neuroblastoma cells incubated for 1 h with preformed amylin aggregates (A–D) or Aβ1–42 oligomers (E–H) were surface labeled with anti-amylin (A) or anti-Aβ1–42 (B), respectively, and secondary Alexa 488 conjugated antibodies (green). Single GM1 molecules were detected using biotin-ctxb coupled to streptavidin-QD 655 (A and E, red). (B and F) Magnification of the white regions in A and E showing the trajectories of GM1 molecules superimposed to the color intensity map of amyloid aggregates. Scale bar, 1 µm. Position vector (C and G) and MSD (D and H) analysis of the GM1 molecules indicated by the coloured arrows in A and E. Colors corresponds to changes from Brownian or directed (red) to confined motion (blue) of a GM1 molecule after interaction with an amyloid aggregate. Orange, control GM1 molecule following typical Brownian motion. The MSD was calculated over the time indicated according to the colors in (C).

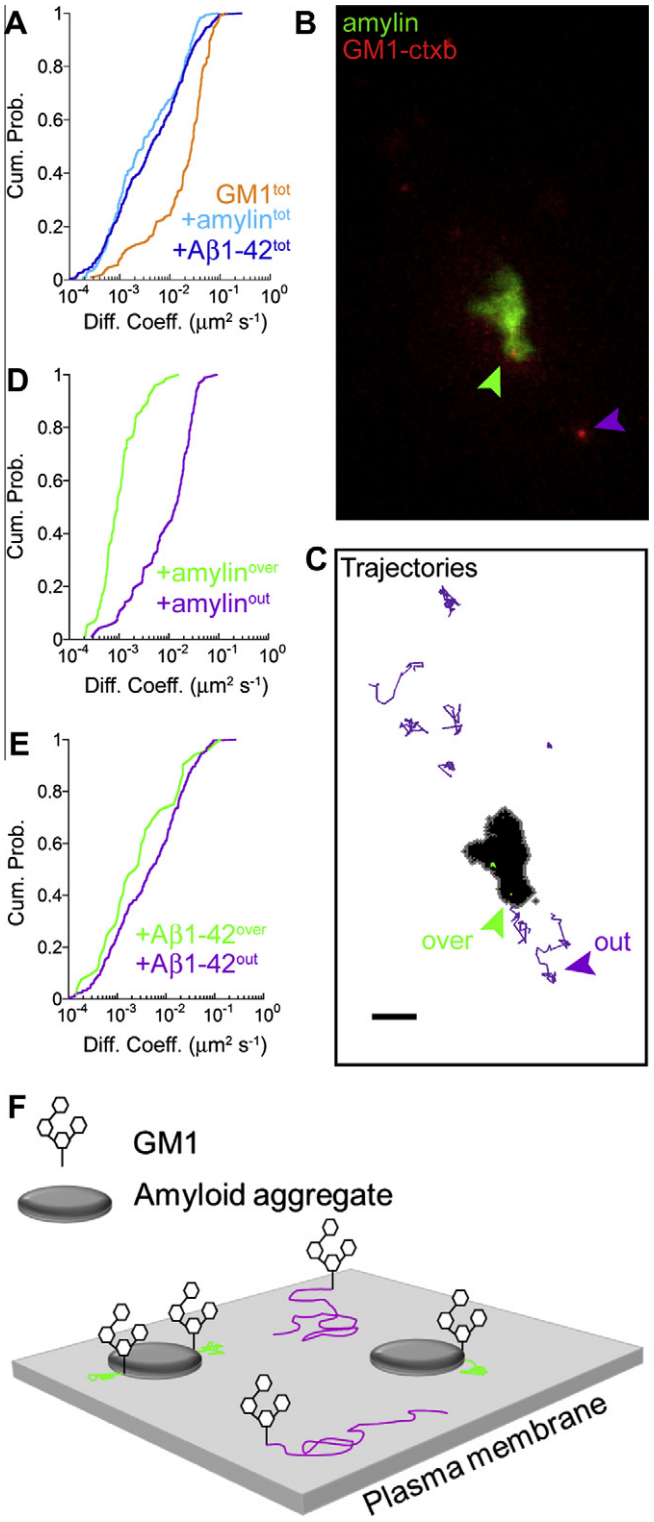

Fig. 3. Amyloid aggregates cause the confinement of a subpopulation of GM1 molecules. (A) The cumulative probability distributions of GM1 diffusion coefficients in cells incubated for 1 h with preformed amylin aggregates (cyan) and Aβ1–42 oligomers (blue) show a decreased mobility as compared to control cells (orange). (B and C) Example of GM1 trajectories superimposed to binary images of amylin aggregates in a living neuroblastoma cell labeled with anti-amylin, secondary Alexa 488 antibodies and biotin-ctxb coupled to streptavidin-QD 655. Trajectories were classified as over (green) and apart (purple) from amylin aggregates. Scale bar, 2 μm. (D and E) Cumulative *D* values distributions of QD-coupled GM1 calculated from trajectories located over and apart from amylin aggregates (D) or Aβ1–42 oligomers (E). (F) Schematic representation of amyloid aggregates affecting the lateral diffusion of GM1 molecules.

Table 1
Amylin aggregates and Aβ1–42 oligomers alter the lateral diffusion of GM1-ctxb on the plasma membrane of SH-SY5Y neuroblastoma cells.

Condition	D_{median} ($\mu m^2 s^{-1}$)	Δ_{max} [a]	P [b]
GM1-ctxb	2.70×10^{-2}		
GM1-ctxb + amylin tot	2.94×10^{-3}	4.4×10^{-1}	$\leqslant 10^{-4}$
GM1-ctxb + Aβ1–42 tot	4.17×10^{-3}	4.1×10^{-1}	$\leqslant 10^{-4}$
GM1-ctxb + amylin out	1.34×10^{-2}	3.2×10^{-1}	$\leqslant 10^{-4}$
GM1-ctxb + amylin over	9.16×10^{-4}	7.7×10^{-1}	$\leqslant 10^{-4}$
CTXB + Aβ1–42 out	4.78×10^{-3}	4.0×10^{-1}	$\leqslant 10^{-4}$
GM1-ctxb + Aβ1–42 over	2.49×10^{-3}	5.1×10^{-1}	$\leqslant 10^{-4}$
Aβ1–42 [26]	6.1×10^{-4}		

[a] Maximum difference in cumulative fraction between cells incubated with and without aggregates.
[b] Kolmogorov–Smirnov test P value calculated using Δ_{max} as statistic. $52 > n > 370$.

tions (2.70×10^{-2} $\mu m^2 s^{-1}$) was found to be in agreement with previous experiments on GM1-ctxb mobility (1.83×10^{-2} $\mu m^2 s^{-1}$ [27], 4.7×10^{-2} $\mu m^2 s^{-1}$ [28]). In cells exposed to amylin aggregates or Aβ1–42 oligomers the cumulative distributions of *D* values appeared to be dramatically different from control experiments (Fig. 3A). The median *D* was one order of magnitude lower either in the presence of amylin aggregates or Aβ1–42 oligomers (Table 1).

Furthermore, when binary masks corresponding to the thresholded fluorescently labeled aggregates were used to discriminate GM1 molecules over and apart from the aggregates (Fig. 3B and C), the distributions and median *D* changed even further (Fig. 3D,E and Table 1). In the case of amylin, the ensemble of molecules localized over amylin aggregates showed a decrease in median *D* of two orders of magnitude compared to the median *D* value of GM1 molecules apart from the aggregates, which in turn resulted to be very similar to the control. In the case of Aβ1–42 the *D* distributions of GM1 over and apart from the oligomers appear not to differ significantly. This result can be explained by the much smaller size of Aβ1–42 oligomers compared to the large amylin aggregates. The low intensity fluorescence signal coming from these small oligomers might have been indistinguishable from background fluorescence, resulting in a biased *D* values distribution of GM1 molecules classified as apart from the oligomers. The median *D* of GM1 over Aβ1–42 oligomers is close to that found for single Aβ oligomers [26] (Table 1).

These results indicate that a subpopulation of GM1 molecules in contact with amyloid aggregates switches its dynamic behaviour to a slower regime (Fig. 3F).

4. Discussion

By combining PLA and SPT experiments, we demonstrate that the changes in mobility of GM1 observed in living cells are effectively a consequence of the interaction with very slow diffusing amyloid aggregates. Our new findings based on the localization of GM1 over and apart from the aggregates provide the rational to explain previous results showing that the overall diffusion of GM1 was decreased in cells exposed to aggregates formed by an amyloidogenic prion protein not associated to any disease [29]. Altogether, these results underline the generic nature of the interaction between amyloid species and GM1 gangliosides.

Previous results in fixed cells have suggested that Aβ oligomers can be trafficked on the plasma membrane and accumulate in lipid rafts [12,17]. Williamsons and co-workers [17] show a higher degree of co-localization of GM1 and exogenously added Aβ oligomers after 1 h incubation compared to 1 min, and suggest that lipid rafts act as sites of Aβ accumulation. What we observed with real time imaging of GM1 indicates however a substantial differ-

ence: apparently, Aβ1–42 changes the dynamics of GM1, and possibly of membrane rafts, as a consequence of their interaction. We found that GM1 follows the lateral diffusion behaviour of Aβ1–42 oligomers [26], not the inverse. Nonetheless, while demonstrating that GM1 molecules are sequestered by amyloid aggregates, our results do not exclude further clustering of GM1 and aggregates at later stages.

Our results give rise to additional considerations. While plasma membrane permeation and deformation have been the subject of many studies, impairment and dysfunction caused by changes in mobility and lateral trafficking of membrane molecules induced by amyloid aggregates have been poorly investigated. Considering that amyloids can bind to a large number of biological molecules that range from glycosaminoglycans and nucleic acids to a variety of proteins and lipids, the change in membrane dynamics observed for GM1 may imply that amyloids can potentially harm all those cellular mechanisms that base their efficiency on molecules mobility. Although here we limited our investigation to GM1, growing evidence shows that amyloid aggregates can alter the membrane mobility of a number of proteins and other plasma membrane components, and lead either to a gain or to a loss of function. For example, the binding of Sup35 amyloid fibrils to the plasma membrane can possibly cause an accumulation of Fas receptors associated with GM1 with subsequent activation of extrinsic apoptotic pathways [29]. On the other hand, sequestration of neurotransmitter receptors, such as the metabotropic glutamate mGluR5, by Aβ1–42 oligomers has been shown to impair intracellular calcium levels and synaptic network activity [33]. Within this context, an alteration of GM1 mobility may compromise its regulatory role in neurodevelopment and neuroprotection [34,35], or influence cellular pathways linked to raft dynamics.

Acknowledgements

We thank M. Capitanio and L. Gardini for technical advice and assistance, F. Vanzi, B. Bisel, M. Bucciantini and M. Stefani for critical discussions. This work was supported by the European Union Seventh Framework Programme (FP7/2007–2013) under grant agreements No. 228334 and PIEF-GA-2009-254791, the Italian Ministry for Education, University and Research in the framework of the Flagship Project NANOMAX, the European Union Seventh Framework Programme (FP7/2007–2013) under grant agreement No.284464 and the Ente Cassa di Risparmio di Firenze (private foundation).

Appendix A. Supplementary data

Supplementary data associated with this article can be found, in the online version, at http://dx.doi.org/10.1016/j.febslet.2013.03.014.

References

[1] Sakono, M. and Zako, T. (2010) Amyloid oligomers: formation and toxicity of Abeta oligomers. FEBS J. 277 (6), 1348–1358.
[2] McLaurin, J. and Chakrabartty, A. (1996) Membrane disruption by Alzheimer beta-amyloid peptides mediated through specific binding to either phospholipids or gangliosides. Implications for neurotoxicity. J. Biol. Chem. 271 (43), 26482–26489.
[3] Yanagisawa, K. (2007) Role of gangliosides in Alzheimer's disease. Biochim. Biophys. Acta 1768 (8), 1943–1951.
[4] Cecchi, C. et al. (2009) A protective role for lipid raft cholesterol against amyloid-induced membrane damage in human neuroblastoma cells. Biochim. Biophys. Acta 1788 (10), 2204–2216.
[5] Matsuzaki, K., Kato, K. and Yanagisawa, K. (2010) Abeta polymerization through interaction with membrane gangliosides. Biochim. Biophys. Acta 1801 (8), 868–877.
[6] Evangelisti, E. et al. (2012) Membrane lipid composition and its physicochemical properties define cell vulnerability to aberrant protein oligomers. J. Cell Sci. 125 (Pt 10), 2416–2427.
[7] Lingwood, D. and Simons, K. (2010) Lipid rafts as a membrane-organizing principle. Science 327 (5961), 46–50.
[8] Simons, K. and Gerl, M.J. (2010) Revitalizing membrane rafts: new tools and insights. Nat. Rev. Mol. Cell Biol. 11 (10), 688–699.
[9] Pernber, Z. et al. (2012) Altered distribution of the Gangliosides GM1 and GM2 in Alzheimer's disease. Dement. Geriatr. Cogn. Disord. 33 (2–3), 174–188.
[10] Kurganov, B., Doh, M. and Arispe, N. (2004) Aggregation of liposomes induced by the toxic peptides Alzheimer's Abetas, human amylin and prion (106–126): facilitation by membrane-bound GM1 ganglioside. Peptides 25 (2), 217–232.
[11] Gellermann, G.P. et al. (2005) Raft lipids as common components of human extracellular amyloid fibrils. Proc. Natl. Acad. Sci. USA 102 (18), 6297–6302.
[12] Wakabayashi, M. and Matsuzaki, K. (2009) Ganglioside-induced amyloid formation by human islet amyloid polypeptide in lipid rafts. FEBS Lett. 583 (17), 2854–2858.
[13] Engel, M.F. (2009) Membrane permeabilization by Islet amyloid polypeptide. Chem. Phys. Lipids 160 (1), 1–10.
[14] Ikeda, K. et al. (2011) Mechanism of amyloid beta-protein aggregation mediated by GM1 ganglioside clusters. Biochemistry 50 (29), 6433–6440.
[15] Okada, T. et al. (2008) Formation of toxic Abeta(1–40) fibrils on GM1 ganglioside-containing membranes mimicking lipid rafts: polymorphisms in Abeta(1–40) fibrils. J. Mol. Biol. 382 (4), 1066–1074.
[16] Wakabayashi, M. et al. (2005) GM1 ganglioside-mediated accumulation of amyloid beta-protein on cell membranes. Biochem. Biophys. Res. Commun. 328 (4), 1019–1023.
[17] Williamson, R. et al. (2008) Membrane-bound beta-amyloid oligomers are recruited into lipid rafts by a fyn-dependent mechanism. FASEB J. 22 (5), 1552–1559.
[18] Williams, T.L. et al. (2011) Abeta42 oligomers, but not fibrils, simultaneously bind to and cause damage to ganglioside-containing lipid membranes. Biochem. J. 439 (1), 67–77.
[19] Bannai, H. et al. (2006) Imaging the lateral diffusion of membrane molecules with quantum dots. Nat. Protoc. 1 (6), 2628–2634.
[20] Bonneau, S., Dahan, M. and Cohen, L.D. (2005) Single quantum dot tracking based on perceptual grouping using minimal paths in a spatiotemporal volume. IEEE Trans. Image Process. 14 (9), 1384–1395.
[21] Ehrensperger, M.V. et al. (2007) Multiple association states between glycine receptors and gephyrin identified by SPT analysis. Biophys. J. 92 (10), 3706–3718.
[22] Lingwood, D. et al. (2008) Plasma membranes are poised for activation of raft phase coalescence at physiological temperature. Proc. Natl. Acad. Sci. USA 105 (29), 10005–10010.
[23] Saxton, M.J. and Jacobson, K. (1997) Single-particle tracking: applications to membrane dynamics. Annu. Rev. Biophys. Biomol. Struct. 26, 373–399.
[24] Lacor, P.N. et al. (2007) Abeta oligomer-induced aberrations in synapse composition, shape, and density provide a molecular basis for loss of connectivity in Alzheimer's disease. J. Neurosci. 27 (4), 796–807.
[25] Kayed, R. et al. (2007) Fibril specific, conformation dependent antibodies recognize a generic epitope common to amyloid fibrils and fibrillar oligomers that is absent in prefibrillar oligomers. Mol. Neurodegener. 2, 18.
[26] Calamai, M. and Pavone, F.S. (2011) Single molecule tracking analysis reveals that the surface mobility of amyloid oligomers is driven by their conformational structure. J. Am. Chem. Soc. 133 (31), 12001–12008.
[27] Renner, M., Choquet, D. and Triller, A. (2009) Control of the postsynaptic membrane viscosity. J. Neurosci. 29 (9), 2926–2937.
[28] Jones, R. et al. (2010) Tracking diffusion of GM1 gangliosides and *Zona pellucida* binding molecules in sperm plasma membranes following cholesterol efflux. Dev. Biol. 339 (2), 398–406.
[29] Bucciantini, M. et al. (2012) Toxic effects of amyloid fibrils on cell membranes: the importance of ganglioside GM1. FASEB J. 26 (2), 818–831.
[30] Groc, L. et al. (2007) Surface trafficking of neurotransmitter receptor: comparison between single-molecule/quantum dot strategies. J. Neurosci. 27 (46), 12433–12437.
[31] Meier, J. et al. (2001) Fast and reversible trapping of surface glycine receptors by gephyrin. Nat. Neurosci. 4 (3), 253–260.
[32] Calamai, M. et al. (2009) Gephyrin oligomerization controls GlyR mobility and synaptic clustering. J. Neurosci. 29 (24), 7639–7648.
[33] Renner, M. et al. (2010) Deleterious effects of amyloid beta oligomers acting as an extracellular scaffold for mGluR5. Neuron 66 (5), 739–754.
[34] Furukawa, K. et al. (2011) Regulatory mechanisms of nervous systems with glycosphingolipids. Neurochem. Res. 36 (9), 1578–1586.
[35] Yu, R.K., Tsai, Y.T. and Ariga, T. (2012) Functional roles of gangliosides in neurodevelopment: an overview of recent advances. Neurochem. Res. 37 (6), 1230–1244.